Polym. Korea, Vol. 50, No. 3, pp. 423-430 (2026)
https://doi.org/10.7317/pk.2026.50.3.423
ISSN 2234-8077(Online)

PVC/BP-264 기반 폴리머의 합성 및 항균 특성 평가

Thi Thanh Huyen Nguyen†, Dinh Nhi Bui*,†, and Thi Thao Minh**,†
Faculty of Chemical Engineering, Viet Tri University of Industry
*Faculty of Natural Sciences, Electric Power University
**Faculty of New Energy, Electric Power University
(2025년 10월 29일 접수, 2026년 1월 31일 수정, 2026년 3월 3일 채택)

Synthesis and Evaluation of Antibacterial Properties of PVC/BP-264-Based Polymer

Thi Thanh Huyen Nguyen†, Dinh Nhi Bui*,†, and Thi Thao Minh,†**
Faculty of Chemical Engineering, Viet Tri University of Industry, Phu Tho, Vietnam
**Faculty of Natural Sciences, Electric Power University, 235 Hoang Quoc Viet Street, Co Nhue 1Ward, Bac Tu Liem District, Hanoi City, 11917, Vietnam*
***Faculty of New Energy, Electric Power University, 235 Hoang Quoc Viet Street, Co Nhue 1Ward, Bac Tu Liem District, Hanoi City, 11917, Vietnam*
(Received October 29, 2025; Revised January 31, 2026; Accepted March 3, 2026)

Abstract: In this study, an antibacterial polymer was successfully synthesized by copolymerization using poly(vinyl chloride) (PVC) and 2,2',6,6'-tetra-tert-butyl-4,4'-dihydroxybiphenyl (BP-264). Covalent incorporation was supported by Fourier transform infrared spectroscopy (FTIR), UV–Vis spectroscopy (appearance of a BP-264 absorption band near 295 nm in PVC–BP-264), and $^{1}H/^{13}C$ nuclear magnetic resonance (NMR) spectra with corrected chemical-shift assignments for tert-butyl, aromatic, and phenolic signals. GPC showed a modest change in molecular-weight distribution after modification (M_n 4.60×10^4 g mol^{-1}, M_w 9.40×10^4 g mol^{-1}). Mechanical testing demonstrated improved ductility while maintaining strength: PVC–BP-264 reached a tensile strength of about 19 MPa and elongation at break of about 270%, accompanied by a slight decrease in modulus to about 1.9 GPa. Preliminary antibacterial screening by agar disk diffusion against Escherichia coli and Staphylococcus aureus revealed clear growth-inhibition zones for PVC–BP-264 compared with PVC. Overall, this study provides a chemistry-driven route to antibacterial PVC with a favorable balance of mechanical performance.

Keywords: poly(vinyl chloride), 2,2',6,6'-tetra-tert-butyl-4,4'-dihydroxybiphenyl, antibacterial polymer, phenolic modification, thermal stability.

Introduction

Microbial contamination of contact surfaces, from medical devices to food packaging to water treatment infrastructur, remains a global challenge as bacteria such as *E. coli* and *S. aureus* adhere, form biofilms, and develop antibiotic resistance. In this context, antimicrobial polymers have emerged as a platform that is customizable (contact action, agent release, surface modification), stable, processable, and suitable for large-scale deployment.[1] Typical mechanisms of action include (i) membrane disruption *via* structurally optimized cationic/hydrophobic groups, (ii) use-as-you-go release of agents (metal ions, active molecules, ROS), and (iii) anti-adhesion to prevent biofilm formation; strategies can be combined to create synergistic effects in biomedical devices and surfaces.[2] However, recent reviews have also warned of the risk of tolerance/resistance selection when overusing some antimicrobial coatings (especially silver/copper and peptides) in healthcare settings, calling for rigorous evaluation of long-term safety and the risk of resistance gene co-selection.[3]

Poly(vinyl chloride) (PVC) is one of the most important industrial polymers due to its mechanical and chemical stability, ease of processing, and low cost; however, virgin PVC has

†To whom correspondence should be addressed.
huyenntt@vui.edu.vn, ORCID 0009-0003-7118-613X
nhibd@epu.edu.vn, ORCID 0000-0002-7238-6585
thaomt@epu.edu.vn, ORCID 0009-0003-0226-1247

limited antibacterial activity. Three approaches have proven effective: (i) surface functionalization/grafting with bactericidal groups (guanidine, quaternary ammonium), which provides in situ bactericidal activity and biofilm inhibition; (ii) loading/anchoring agents such as NO donors (SNAPs) into the PVC matrix to create a durable self-antibacterial surface; and (iii) composites with inorganic/organic phases, adjusting surface morphology and release kinetics.[4] Specifically, guanidine-containing polymer-coated PVC provides broad Gram-positive/negative efficacy and significantly reduces adhesion; cationic PVC (quaternary ammonium group) achieves pathogen inactivation by in situ contact mechanism; and SNAP-coated PVC provides stable NO release in biomedical devices (tubes, ETT) while still controlling leakage thanks to biocompatible coatings.[5–8] More broadly, studies of intrinsic antimicrobial polymers and coatings in food/biomedical applications confirm the pivotal role of positive charge density, hydrophilic-hydrophobic balance, and chain architecture in efficacy—while also highlighting the optimization problem of preserving biocompatibility, mechanical properties, and durability.[5,9]

A prominent research gap is the absence of data extrapolated to real-world conditions (abrasion-cleaning-disinfection cycles, complex biological fouling), standardization of testing (cross-strain/condition comparisons), and long-term evaluation of thermal-optic-mechanical stability as well as safety/environmental (leaching, toxicity). Against this background, the combination of PVC backbones with phenolic units (*e.g*., biphenyl dihydroxy) promises to create surfaces that are less sticky and/or less likely to engage in unfavorable physicochemical interactions with bacteria, while retaining the processing advantages and durability of PVC. Therefore, this study aimed to copolymerize/graft PVC with BP-264, then verify the structure (FTIR, NMR), thermal stability (TGA), morphology (SEM), and antibacterial activity against *E. coli* and *S. aureus*, compared with control samples and solvent references, as a small but practical step towards a practically deployable antibacterial polymer coating.

Experimental

Materials and Chemicals. Poly(vinyl chloride) (PVC, average $M_w \approx 62000$, ≥99% purity; Sigma–Aldrich, USA) and 2,2',6,6'-tetra-tert-butyl-4,4'-dihydroxybiphenyl (BP-264, 99%; Sigma–Aldrich, USA) were used as received without further purification. Tetrahydrofuran (THF), triethylamine (TEA, ≥99%), and potassium iodide (KI, ≥99.5%) were obtained from Sigma–Aldrich, USA and used directly.

Method of Manufacturing Polymer PVC-BP-264. PVC-BP-264 was prepared as follows (Scheme 1). PVC (0.645 g) and BP-264 (1.98 g) were dissolved in tetrahydrofuran (THF, ~50 mL) under stirring to obtain a homogeneous solution. Potassium iodide (KI, 0.5 mL) and triethylamine (TEA, 1.0 mL) were then added dropwise; KI acted as an iodide promoter and TEA as an acid scavenger to facilitate the subsequent coupling. The mixture was refluxed at 100 °C for 24 h. After reaction, the product was precipitated into water, collected by filtration (Whatman paper), washed thoroughly with THF to remove unreacted species/by-products, and air-dried at room temperature to afford a pale-yellow PVC-BP-264 solid.

Gel Permeation Chromatography (GPC). Gel permeation chromatography was performed to determine the molecular-weight distribution of PVC and PVC–BP-264. Samples were dissolved in tetrahydrofuran (THF) to a concentration of 2.0 mg mL^{-1}, filtered through a 0.45 μm PTFE syringe filter, and injected (100 μL). The measurements were carried out using a conventional GPC system (Agilent 1260 Infinity II, Agilent Technologies, USA) equipped with a refractive index (RI) detector and two mixed-bed SEC columns (5 μm, 300 × 7.5 mm) with a corresponding guard column. The column oven was maintained at 35 °C and THF was used as the mobile phase at a flow rate of 1.0 mL min^{-1}. The system was calibrated using narrow polystyrene standards. Number-average molecular weight (M_n) and weight-average molecular weight (M_w) were calculated from the chromatograms.

Material Properties. FTIR spectra were collected over the range of 4000-400 cm^{-1} using an FTIR spectrometer (Nicolet

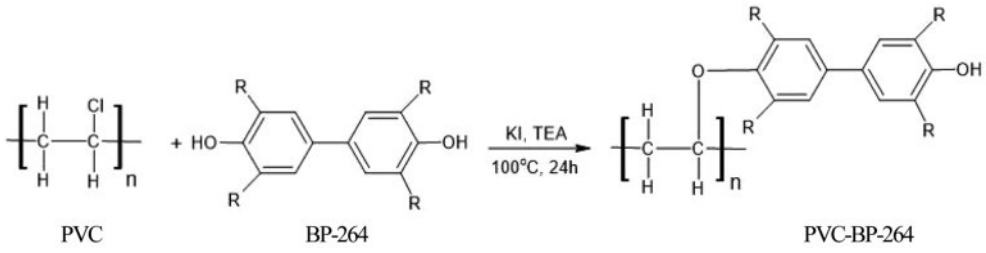

Scheme 1. PVC-BP-264 synthesis process.

iS10, Thermo Fisher Scientific, USA), and baseline corrections were applied as needed to compare PVC, BP-264, and PVC-BP-264. Proton and carbon NMR spectra (^{1}H 400 MHz and ^{13}C 100 MHz, DMSO-d_6) were recorded using an NMR spectrometer (Bruker Avance III 400 MHz, Bruker, Germany) and processed with standard phase and baseline corrections, apodization, zero-filling, and signal integration to assign aromatic and backbone resonances. Thermogravimetric analysis (TGA) was performed on approximately 10 mg samples over the temperature range of 25-800 °C at a heating rate of 5 °C min^{-1} under a nitrogen atmosphere using a thermogravimetric analyzer (TGA Q500, TA Instruments, USA). Surface morphology was examined by scanning electron microscopy (SEM) using a field-emission SEM instrument (JSM-7600F, JEOL Ltd., Japan) operated at an accelerating voltage of 10 kV across multiple magnifications. The samples were sputter-coated with palladium (Pd) when necessary to reduce surface charging, and representative micrographs were analyzed to evaluate feature dispersion. UV−Vis spectroscopy was used to confirm the presence of BP-264 chromophores in the modified PVC. Solutions of PVC, BP-264, and PVC-BP−264 were prepared in THF at a concentration of 0.10 mg mL^{-1} and recorded using a UV−Vis spectrophotometer (UV-2600, Shimadzu Corporation, Japan) equipped with a 1 cm quartz cuvette. Spectra were recorded from 200 to 800 nm with a scan interval of 1 nm. Tensile properties were measured using a universal testing machine (Galdabini Quasar 5 kN, Italy) at room temperature. Dumbbell-shaped specimens were cut from solvent-cast films and tested at a constant crosshead speed of 10 mm min^{-1} with a gauge length of 20 mm. Young's modulus was determined from the initial linear region of the stress–strain curve, and tensile strength and elongation at break were obtained from the maximum stress and the strain at failure, respectively. At least five specimens were tested for each material, and the mean ± standard deviation.

Evaluation of Antibacterial Ability. The antibacterial performance of PVC-BP-264 was evaluated against *Escherichia coli* (ATCC 25922) and *Staphylococcus aureus* (ATCC 25923) using the Kirby–Bauer disk diffusion method, following CLSI guidelines. Sterile paper disks (6 mm diameter) were impregnated with 20 μL of polymer solution in DMSO (50 mg mL^{-1}), dried under sterile conditions, and placed on Mueller–Hinton agar plates inoculated with bacterial suspensions adjusted to 0.5 McFarland standard (~10^6 CFU mL^{-1}). Control disks included DMSO alone. Plates were incubated at 37 °C for 24 h, after which inhibition zones were measured with a digital caliper in triplicate. Results are reported as mean ± standard deviation. This assay was selected as it is widely used for the preliminary screening of antibacterial polymers.[9]

Results and Discussion

GPC Analysis. The GPC chromatograms of neat PVC and PVC–BP-264 display a dominant, essentially unimodal peak at a very similar retention time (≈13–14 min), indicating that the overall molecular-weight distribution of the PVC backbone is largely preserved after functionalization (Figure 1). At the same time, the molecular-weight averages increase from M_n = 35043 and M_w = 80613 g·mol^{-1} (PVC) to M_n = 45957 and M_w = 94005 g·mol^{-1} (PVC–BP-264). Because GPC separates by hydrodynamic size, the modest increase in M_n/M_w together with the similar peak shape is consistent with successful incorporation of BP-264 without introducing a strongly broadened distribution.[10] In contrast, pronounced chain scission typically manifests as a clear drop in molecular weight (often with increased low-molar-mass contribution), whereas extensive crosslinking tends to generate very high-molar-mass fractions and marked peak broadening.[11]

Characteristics of Polymer Materials. The FTIR spectrum (Figure 2) of neat PVC displays typical bands at 2960–2870 cm^{-1} (aliphatic C–H stretching), ~1425 cm^{-1} (CH_2 bending), and ~690 cm^{-1} (C–Cl stretching).[12] BP-264 shows a broad O–H band centered at ~3500 cm^{-1}, aromatic C=C vibrations at ~1600 and ~1500 cm^{-1}, and a phenolic Ar–O stretching band near ~1260 cm^{-1}.[13] After modification, PVC–BP-264 exhibits the characteristic PVC bands together with the BP-264-related aromatic/O–H/Ar–O features, indicating the presence of BP-264 motifs in the modified polymer. The observed pattern therefore sup-

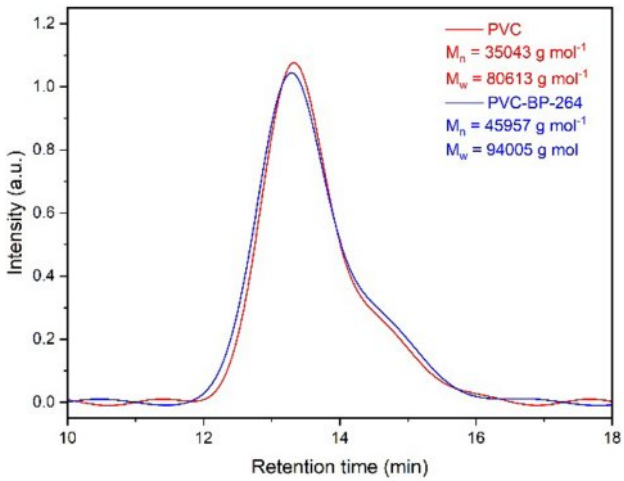

Figure 1. GPC chromatograms of neat PVC and PVC–BP-264.

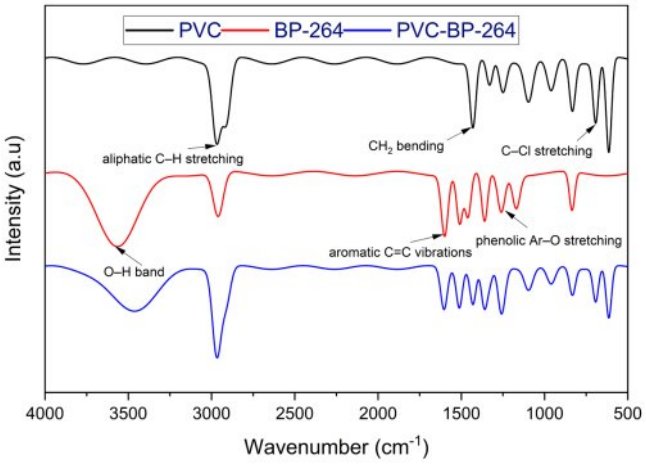

Figure 2. FTIR spectra of PVC, BP-264, and PVC-BP-264.

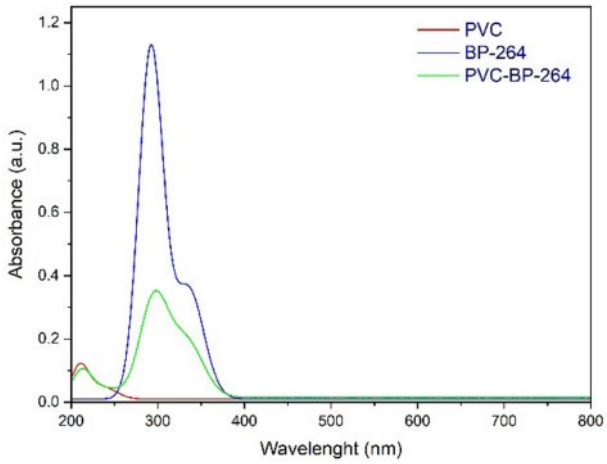

Figure 3. UV-Vis spectra of PVC, BP-264, and PVC-BP-264.

ports substitution at PVC sites and formation of PVC-BP-264 linkages.

As shown in Figure 3, neat PVC exhibits only weak absorption in the deep-UV region with a maximum near ~208 nm, which is consistent with the limited intrinsic chromophores of PVC in dilute solution. In contrast, BP-264 shows a strong absorption band with $\lambda_{max} \approx 291$ nm and a broader shoulder band around ~320 nm, characteristic of aromatic phenolic chromophores. The modified polymer (PVC–BP-264) displays the BP-264-related features as a broadened band with $\lambda_{max} \approx 296$ nm and a shoulder near ~320 nm, while retaining the weak deep-UV response of PVC. The emergence of these BP-264-type absorption bands in PVC–BP-264 supports successful incorporation of BP-264 chromophores into the polymer. The substantially lower absorbance of PVC–BP-264 compared with free BP-264 at the same mass concentration is expected because

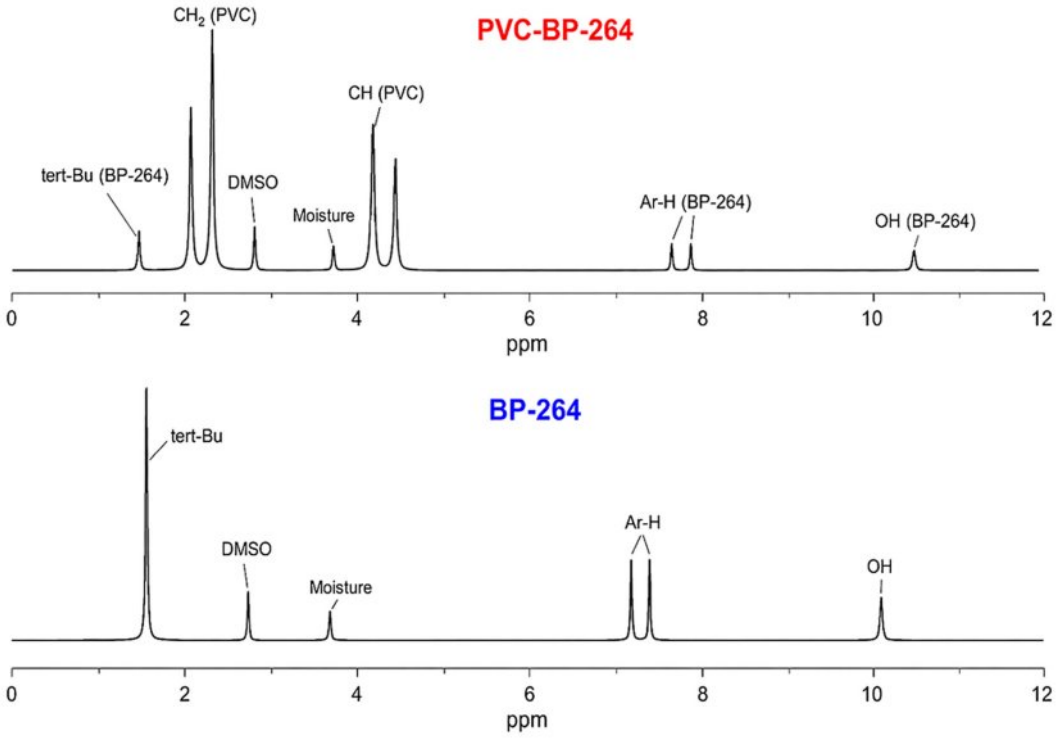

Figure 4. ^{1}H NMR spectra of BP-264 and PVC-BP-264.

the chromophore represents only a fraction of the polymer mass.[14]

In the ^{1}H NMR spectra (Figure 4), BP-264 shows the expected features of a hindered bisphenolic structure: a dominant tert-butyl singlet at about 1.2–1.4 ppm (tert-Bu CH_3), aromatic protons clustered at 6.9–7.3 ppm, and a phenolic OH signal in the downfield region around 9.5–10.0 ppm (often broad, depending on H-bonding and moisture). In the PVC–BP-264 spectrum, the polymer backbone gives broad resonances typical of PVC, namely –CH_2– signals in the 2.5–1.9 ppm region and –CHCl– signals in the 4.6–3.9 ppm region; these are known PVC chemical-shift windows and commonly appear broadened due to the macromolecular environment.[15] Superimposed on the PVC envelope, the appearance of BP-264-derived signals (tert-Bu near ~1.3 ppm and Ar-H near ~7.0 ppm) supports incorporation of BP-264 moieties into the PVC matrix rather than neat PVC alone.

In the ^{13}C NMR (Figure 5), BP-264 displays characteristic tert-butyl carbon signals (~30–32 ppm for tert-Bu CH_3 and ~34–36 ppm for the tert-Bu quaternary carbon, Cq), together with aromatic carbons spanning roughly ~118–145 ppm and more downfield phenolic Ar–C–O carbons around ~150–156 ppm. For PVC–BP-264, the spectrum contains the broad PVC backbone carbon resonances alongside the additional aromatic/tert-butyl carbons attributable to BP-264, giving a combined pattern consistent with BP-264 functionality present on or within the polymer. Overall, the coexistence of PVC backbone signals with the new BP-264 aromatic/tert-butyl features in both ^{1}H and ^{13}C NMR is consistent with successful BP-264 introduction to PVC.

Thermogravimetric analysis (TGA) of PVC-BP-264 shows multi-step mass loss with discernible events near ~170–220, ~280–300 °C, and a major stage at ~430 °C (Figure 6). For comparison, neat PVC typically undergoes two principal steps under inert atmosphere: an early dehydrochlorination (≈200–320 °C) followed by further backbone scission/aromatization at higher temperatures (≈370–480 °C), with details depending on formulation and heating rate. The upward shift of the main mass-loss temperature in our copolymer toward ~430 °C is consistent with enhanced thermal stability, plausibly due to the rigid, sterically protected BP-264 segments (tetra-tert-butyl biphenyl) that can hinder chain mobility and delay scission. Similar stabilization, manifested as delayed onset or higher T_{max}, has been observed when PVC is endowed with robust aromatic/heteroatom functionalities or when stabilizing moieties are introduced; conversely, conditions that catalyze dehydrochlorination typi-

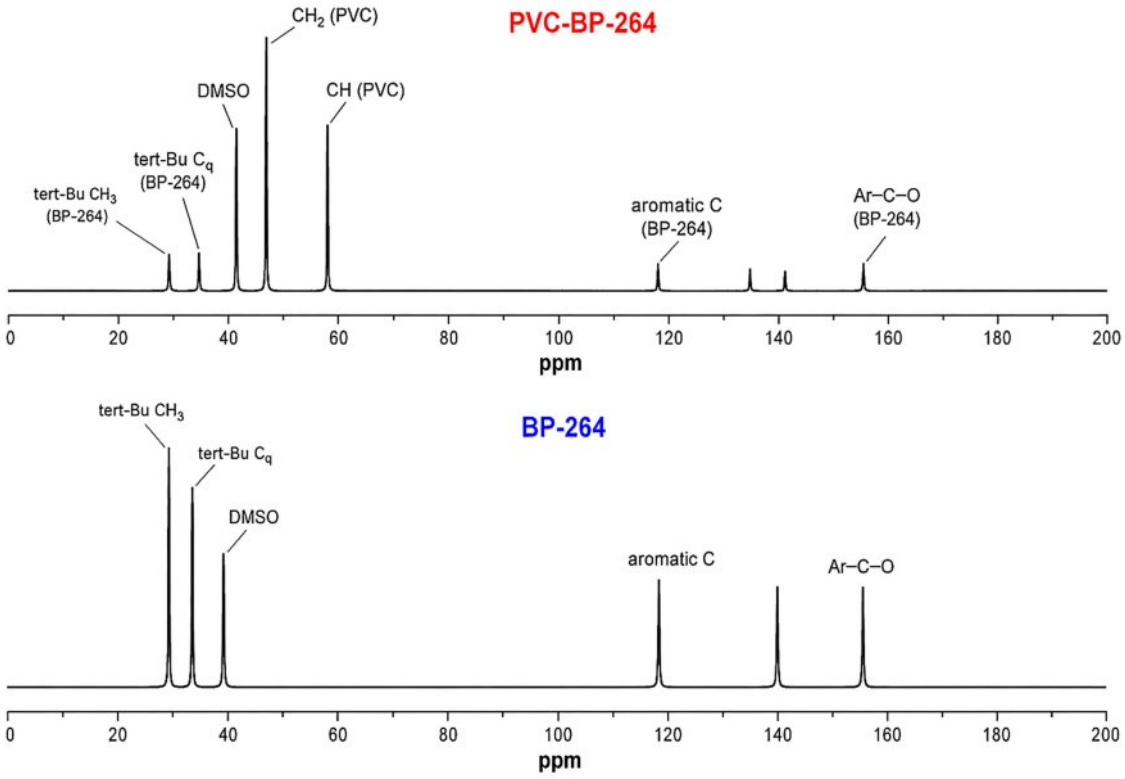

Figure 5. ^{13}C NMR spectra of BP-264 and PVC-BP-264.

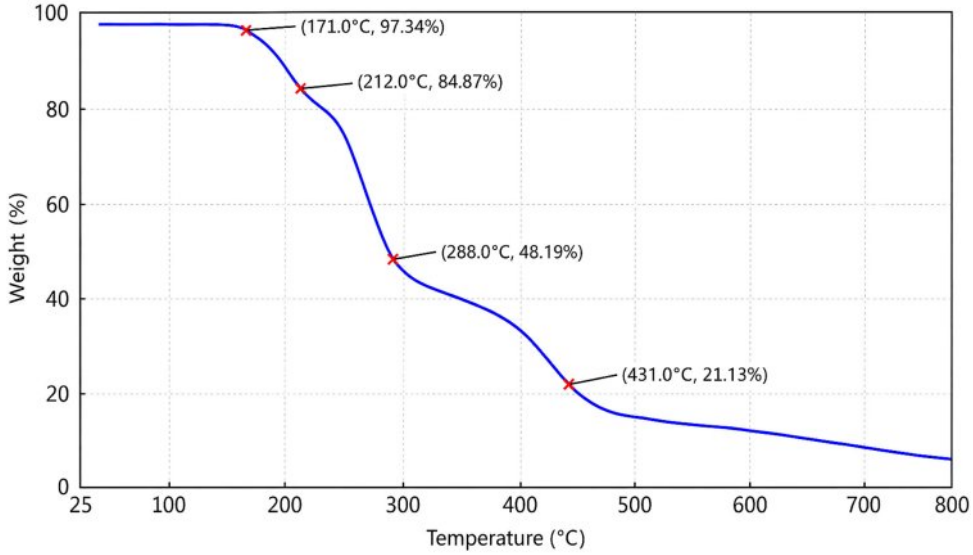

Figure 6. TGA curve of PVC-BP-264.

cally lower the onset (*e.g.*, acidic additives). Thus, the PVC-BP-264 profile aligns with the canonical PVC degradation mechanism while evidencing a net stabilizing effect relative to unmodified PVC.[16]

The surface morphology study of PVC-BP-264 polymer is shown in Figure 7. The results of the surface analysis of the material show a seemingly random and uniform dispersion of particles on the surface of the material. This uniform dispersion significantly enhances the mechanical flexibility of the material, significantly reducing its susceptibility to structural failures such as cracking or peeling. Therefore, the surface morphology analysis highlights the great potential of the material for diverse applications.

Mechanical testing (Figure 8) shows that neat PVC exhibits a Young's modulus of about 2.3 GPa, a tensile strength of about 16.2 MPa, and an elongation at break of about 210%, reflecting the typical balance of stiffness and ductility for plasticized/processable PVC. In contrast, BP-264 alone behaves as a stiff and brittle organic solid, with a higher modulus of about 3.2 GPa but a much lower tensile strength of about 9.6 MPa and a very limited elongation at break of about 4%, consistent with a rigid aromatic small molecule that fractures with minimal plastic deformation. After chemical incorporation of BP-264, the PVC–BP-264 sample displays a lower modulus of about 1.9 GPa together with an increased tensile strength of about 19.0 MPa and a higher elongation at break of about 270%, indicating a clear improvement in toughness and flexibility relative to PVC.

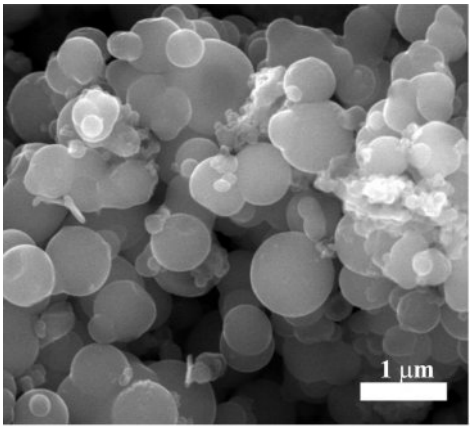

Figure 7. SEM image of PVC-BP-264.

This trend is consistent with an internal-plasticization mechanism: introducing bulky aromatic/phenolic substituents along the PVC backbone can increase free volume and reduce interchain packing, which lowers stiffness and facilitates chain mobility and plastic deformation, while covalent attachment keeps the modifier molecularly dispersed and prevents macrophase separation, enabling efficient stress transfer so that strength is retained or even enhanced. Similar modulus–elongation trade-offs (decreased modulus with increased elongation and tunable strength) have been widely reported for internally plasticized or covalently modified PVC systems prepared via copolymerization or grafting of pendant groups onto PVC to tailor mechanical performance and suppress additive migration.[17,18]

Evaluation of Antibacterial Ability. The antibacterial per-

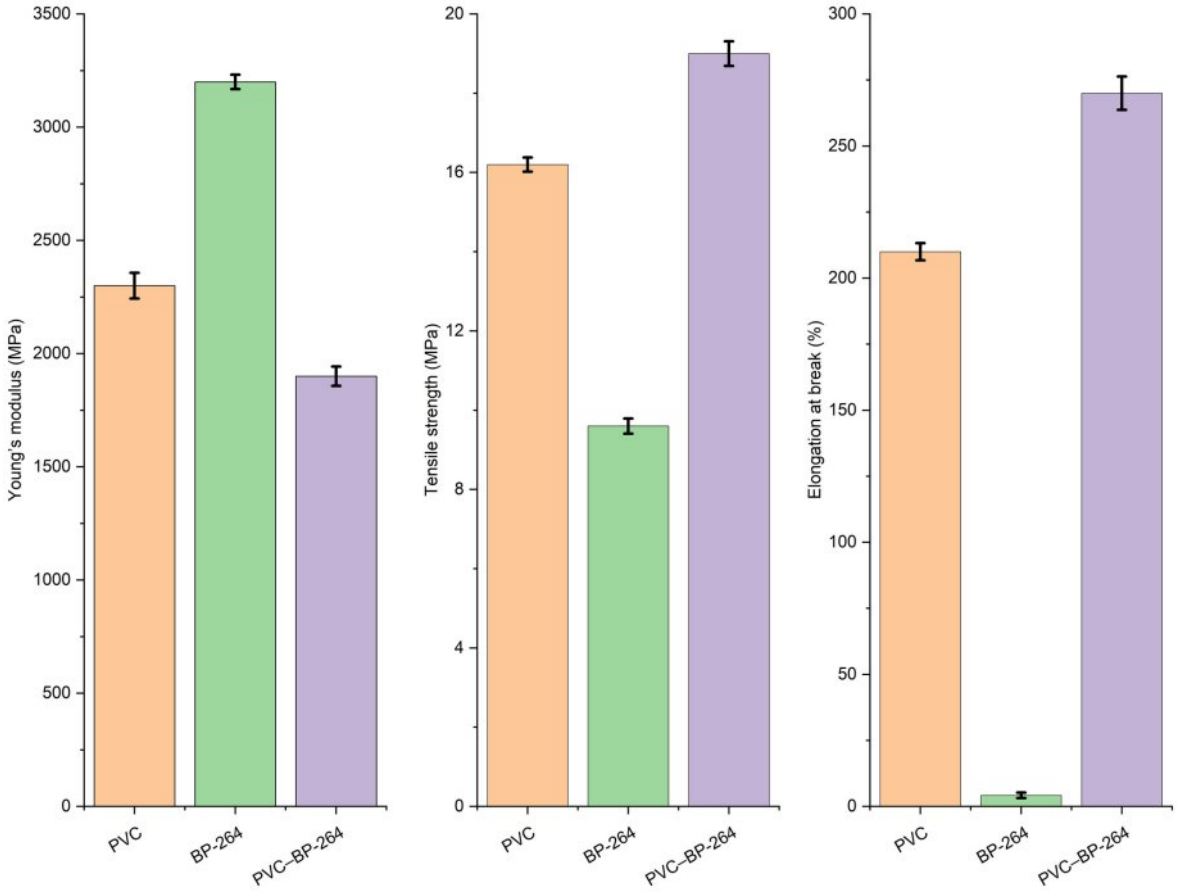

Figure 8. Mechanical properties of BP-264 and PVC-BP-264.

formance of PVC-BP-264 was systematically assessed against *E. coli* (Gram-negative) and *S. aureus* (Gram-positive) using the Kirby–Bauer disk diffusion assay. As shown in Figure 9, the inoculated control plates exhibit confluent bacterial growth, whereas the PVC–BP-264 samples produce a clear growth-inhibition region around the disk for both *E. coli* and *S. aureus*. The inhibition appears more pronounced for *S. aureus* than for *E. coli*, which is commonly observed when comparing Gram-positive and Gram-negative bacteria because the outer membrane of Gram-negative cells can reduce susceptibility to hydrophobic/phenolic agents. This trend aligns with prior reports of functionalized PVC surfaces bearing guanidine or quaternary ammonium groups, which also exhibited stronger inhibition toward *S. aureus*. The enhanced activity after integrating BP-264 into PVC is consistent with a mechanism where BP-264 moieties become concentrated near the polymer interface, increasing the probability of contact-active interactions with bacterial envelopes (membrane disruption and related stress at the surface).

Phenolic biphenyl/bisphenolic motifs are reported to inhibit

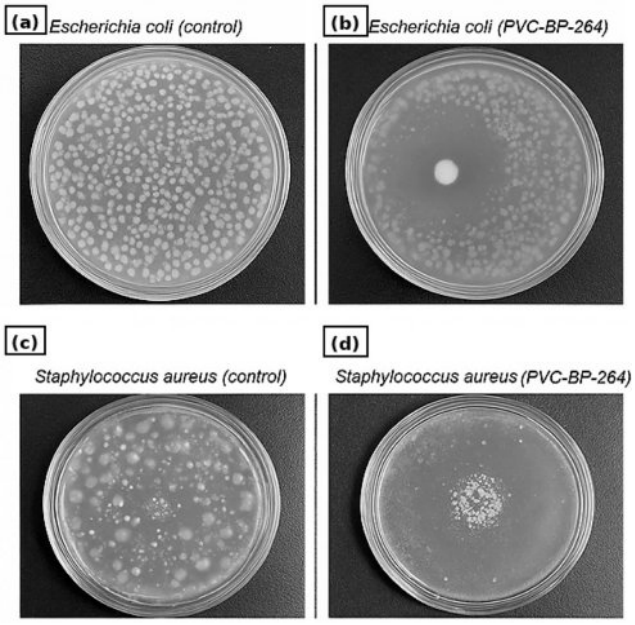

Figure 9. Inhibition of *E. coli* and *S. aureus* by PVC-BP-264 material compared with control samples.

bacterial growth mainly *via* membrane-targeting mechanisms. The hydrophobic aromatic framework (and bulky alkyl substituents) can promote interaction with the lipid bilayer, while phenolic OH groups can perturb membrane potential and increase membrane permeability, leading to leakage of cytoplasmic components and disruption of cellular energetics. In addition, phenolic antimicrobials have been associated with oxidative-stress responses and inhibition of biofilm-related phenotypes in some systems. These mechanisms are consistent with recent reports on antimicrobial phenolic materials and bisphenol derivatives designed as membrane-targeting antibacterial agents.[19,20]

Acknowledgments: We gratefully acknowledge financial support from Electric Power University.

Conflict of Interest: The authors declare that there is no conflict of interest.

References

1. Haktaniyan, M.; Bradley, M. Polymers Showing Intrinsic Antimicrobial Activity. *Chem. Soc. Rev.* **2022**, 51, 8584-8611.
2. Hung, Y.-T.; McLandsborough, L. A.; Goddard, J. M.; Bastarrachea, L. J. Antimicrobial Polymer Coatings with Efficacy against Pathogenic and Spoilage Microorganisms. *LWT* **2018**, 97, 546-554.
3. Pietsch, F.; O'Neill, A. J.; Ivask, A.; Jenssen, H.; Inkinen, J.; Kahru, A.; Ahonen, M.; Schreiber, F. Selection of Resistance by Antimicrobial Coatings in the Healthcare Setting. *J. Hospital Infection* **2020**, 106, 115-125.
4. Ul Haq, I.; Pinto Vieira, R.; Lima, W. G; de Lima, M. E.; Krukiewicz, K. Antimicrobial Polymers: Elucidating the Role of Functional Groups on Antimicrobial Activity. *Arab J. Basic Appl. Sci.* **2024**, 31, 325-344.
5. Hindi, S. S.; Sabir, J. S. M.; Dawoud, U. M.; Ismail, I. M.; Asiry, K. A.; Mirdad, Z. M.; Abo-Elyousr, K. A.; Shiboob, M. H.; Gabal, M. A.; Albureikan, M. O. I.; Alanazi, R. A.; Ibrahim, O. H. M. Nanocellulose-Based Passivated-Carbon Quantum Dots (P-CQDs) for Antimicrobial Applications: A Practical Review. *Polymers* **2023**, 15, 2660.
6. Cottet, C.; Fernández-García, M.; Peltzer, M. A. Evaluation of Different Concentrations of Antimicrobial Quaternary Polymers on the Behavior of Gelatin- and Starch-Based Films. *Polymers* **2024**, 16, 3168.
7. Carrozza, D.; Malavasi, G; Ferrari, E. Very Large Pores Mesoporous Silica as New Candidate for Delivery of Big Therapeutics Molecules, Such as Pharmaceutical Peptides. *Materials* **2023**, 16, 4151.
8. Feit, C. G; Chug, M. K.; Brisbois, E. J. Development of *S* -Nitroso-*N*-Acetylpenicillamine Impregnated Medical Grade Polyvinyl Chloride for Antimicrobial Medical Device Interfaces. *ACS Appl. Bio Mater.* **2019**, 2, 4335-4345.
9. Qiu, H.; Si, Z.; Luo, Y.; Feng, P.; Wu, X.; Hou, W.; Zhu, Y.; Chan-Park, M. B.; Xu, L.; Huang, D. The Mechanisms and the Applications of Antibacterial Polymers in Surface Modification on Medical Devices. *Front. Bioeng. Biotechnol.* **2020**, 8, 00910.
10. Pellegrino Vidal, R. B.; Castañeda, F. N.; Garrido, M. E.; Padró, J. M. Aqueous Size Exclusion Chromatography Applied to Polymer Analysis: Experimental Conditions and Molecular Weight Calibration Curves. *J. Chromatogr. A* **2024**, 1729, 465042.
11. Park, B.; Peterson, G. I. Comparing Molecular Weight Models for Polymer Degradation with Ball-Mill Grinding. *Polym. Degrad. Stab.* **2023**, 218, 110549.
12. Öteyaka, M. Ö.; Öteyaka, H. C. Chemical and Mechanical Properties Analysis of Extruded Polyvinyl Choloride (PVC)/Sepiolite Composite. *Sak. Univ. J. Sci.* **2019**, 23, 633-640.
13. Joshi, R.; Sathasivam, R.; Jayapal, P. K.; Patel, A. K.; Nguyen, B. Van; Faqeerzada, M. A.; Park, S. U.; Lee, S. H.; Kim, M. S.; Baek, I.; Cho, B.-K. Comparative Determination of Phenolic Compounds in Arabidopsis Thaliana Leaf Powder under Distinct Stress Conditions Using Fourier-Transform Infrared (FT-IR) and Near-Infrared (FT-NIR) Spectroscopy. *Plants* **2022**, 11, 836.
14. Kou, M.; Li, K. Graft Reaction of Furfural with Polyvinyl Chloride and Its Effect on Thermal Stability of Polyvinyl Chloride. *Organics* **2025**, 6, 12.
15. Vebr, A.; Dallegre, M.; Autissier, L.; Drappier, C.; Le Jeune, K.; Gigmes, D.; Kermagoret, A. Nitroxide Mediated Radical Polymerization for the Preparation of Poly(Vinyl Chloride) Grafted Poly(Acrylate) Copolymers. *Polym. Chem.* **2022**, 13, 3275-3283.
16. Cruz, P. P. R.; da Silva, L. C.; Fiuza-Jr, R. A.; Polli, H. Thermal Dehydrochlorination of Pure PVC Polymer: Part I—Thermal Degradation Kinetics by Thermogravimetric Analysis. *J. Appl. Polym. Sci.* **2021**, 138, 50598.
17. Song, C.; Zhang, X.; Ma, Y.; Yang, W. Synthesis Internal-Plasticized PVC Copolymer Resin from Industrial Application View: Copolymerization of Vinyl Chloride with Poly(Ethylene Glycol) Monomethyl Ether Methacrylate *via* Suspension Polymerization. *Polymer* **2024**, 290, 126562.
18. Jha, R. K.; Neyhouse, B. J.; Young, M. S.; Fagnani, D. E.; McNeil, A. J. Revisiting Poly(Vinyl Chloride) Reactivity in the Context of Chemical Recycling. *Chem. Sci.* **2024**, 15, 5802-5813.
19. Pan, Z.; Liu, Z.; Yang, S.; Shen, Z.; Wu, Y.; Liu, Y.; Li, J.; Wang, L. Covalent Grafting of Quaternary Ammonium Salt-Containing Polyurethane onto Silicone Substrates to Enhance Bacterial Contact-Killing Ability. *Polymers* **2024**, 17, 17.
20. Gupta, S.; Puttaiahgowda, Y. M.; Kulal, A. Development and Evaluation of Antimicrobial PVC-Grafted Polymer for Enhanced Paint Applications. *RSC Adv.* **2024**, 14, 25669-25677.